







# Smart Monitoring of Sinkhole Formation Using Optic Fibre Technology

Jeandre Labuschagne<sup>1</sup> , Maria Ferentinou<sup>1</sup>  , Michael Grobler<sup>2</sup>,  
and S. W. Jacobsz<sup>3</sup> 

<sup>1</sup> Department of Civil Engineering Science, University of Johannesburg,  
Johannesburg, RSA

labuschagnej93@gmail.com, mferentinou@uj.ac.za

<sup>2</sup> Department of Electrical and Electronic Engineering,  
University of Johannesburg, Johannesburg, RSA

michaelg@uj.ac.za

<sup>3</sup> Department of Civil Engineering, University of Pretoria, Pretoria, RSA

sw.jacobsz@up.ac.za

**Abstract.** Sinkholes are common geohazards, frequently responsible for sudden catastrophic ground collapse. Development on these areas is affected by historic and ongoing geomorphologic processes that may result in surface movements. Centurion and Pretoria in the province of Gauteng, South Africa are large urban environments underlain to a significant extent by dolomitic bedrock and have been affected by sinkhole hazards in the past decades. Sinkholes occur with little or no warning and directly or indirectly affect communities and/or major and minor infrastructure. Thus, effective monitoring would allow for further understanding of the mechanism of occurrence of sinkholes and lead to the development of a potential early-warning system to provide an alarm or a warning of incipient collapse. In the current study, fibre Bragg gratings (FBGs) were used to instrument a reduced-scale model, simulating a sinkhole event. The tests were conducted in a laboratory environment by embedding optic fibre sensors in the soil and inducing failure until critical conditions were reached. FBG sensors were manufactured in various optic fibre cables at predetermined locations. Strain and temperature data were obtained using the FBGs with an optical interrogator. The measurements were recorded simultaneously and in various positions, giving reliable and comparable results. We believe that this is a promising technology that, once expanded to distributed strain measurement on long lengths of optic fibre, would assist local authorities, municipalities and civil protection authorities towards a strategic sinkhole risk management.

**Keywords:** Sinkhole monitoring · Optic fibre sensor technology ·  
Fibre Bragg gratings · Reduced-scale modelling

## 1 Introduction

In South Africa, development on dolomitic terrain is still an open area for research. During the last decades, improvement in sinkhole hazard mapping, sinkhole spatial analysis, identification of causative and triggering factors and production of sinkhole inventories were made.

The South African National Standards for the development on dolomitic land – SANS 1936 (2012) – established requirements that must be met in order to develop on dolomitic land. Although standards development and adaptation, during the last decades, have resulted in reducing sinkhole associated risks, certain areas are still affected regularly by sinkhole events. There is a need to invest in early detection of sinkhole induced failures, which will eventually result in reduced risk to human lives and infrastructure by enabling proactive remediation.

Sinkholes form in an onion-skin peeling fashion as material above a subterranean void falls to the bottom of the cavity, resulting in the cavity migrating upwards [1]. If the material that arches over the cavity becomes too weak to support itself, a collapse will occur which leads to a sinkhole.

In South Africa, most sinkholes form in areas underlain by dolomite bedrock [2] and according to Jennings et al. [1], five requirements must be met in order for a sinkhole to form. These requirements are:

- Adjacent rigid material to form abutments for the roof of the void must be present. Those abutments are provided by dolomite pinnacles or the sides of a steep-sided subsurface canyon. The span must be able to support the bridging material, i.e. with a span which is too large or with material that is too weak, the arch cannot form.
- A condition of arching must develop in the residuum, i.e. a part or all of the vertically acting self-weight must be carried by arching thrusts to the abutments. Complete arching will have occurred when the vertical stress of the inner curve of the arch is zero.
- A void must develop below the arch in the residuum. The void can be quite small.
- A reservoir must exist below the arch to accept the material which is removed to enlarge the void. Some means of transportation of the material, such as flowing water, is also essential.
- When a void of appropriate size has been established in the residuum, some disturbing agency must arise to cause the roof to collapse. The void will move progressively upwards towards the surface.

Most sinkholes form rapidly, unexpected, with little or no visual warning at all. Soga and Schooling [3] reported that it is becoming increasingly important to obtain information from sensors embedded into engineering infrastructure, as well as earth structures to aid in the quantification of the performance of the infrastructure. This is also relevant in the context of sinkholes.

Although the use of optic fibre sensors (OFSs) is not new technology, its use within the geotechnical community is a relatively new concept which competes well with current monitoring techniques since the optical fibre sensors are small, can survive chemically aggressive environments, is immune to electromagnetic interference and

have the advantage that many different sensors can be multiplexed into one optical fibre [4]. Optical fibre sensing techniques are therefore ideal to be used in instability-prone areas since current measurement techniques, such as strain gauges and vibrating wire sensors, have the disadvantage of being vulnerable to electromagnetic interference, poor stability and poor durability [5].

Optic fibre sensor (OFS) monitoring systems can act as real-time early-warning systems, as well as long-term monitoring systems and can accurately measure minute strain differences at various locations along an optic fibre cable [6]. Thus, the origin of small strain changes within geotechnical structures can be continuously monitored and the resultant strain measurements can be used to predict failure or identify localized failure zones.

In a laboratory environment, localized failure zones are often investigated through reduced-scale physical models. The use of reduced-scale physical modelling to model geotechnical problems is experiencing a growing trend within the geotechnical community as prototype structures are often scaled down using similitude laws to simulate a real-life problem [7]. This has the benefits of studying complex, nonlinear geotechnical systems, boundary conditions and phenomena that are otherwise difficult to visualize [8].

Combining the OFSs with reduced-scale physical models, it has been proven by many researchers that OFSs can successfully be used to detect and possibly monitor ground movement [6, 9, 10]. This advantage of OFSs could, however, also be exploited to monitor sinkhole formation.

## 2 Previous Sinkhole Studies

Sinkhole modelling and the formation of sinkholes have been studied by researchers through laboratory studies, field investigations, numerical modelling, as well as through analytical methods.

Laboratory studies are important to select the parameters of the study. Therefore, many studies have been conducted on both large and reduced-scale physical models in a 1-g environment and/or under accelerated gravitational conditions using a geotechnical centrifuge.

Many researchers have documented the sinkhole formation process through physical modelling either in a 1-g environment or in an environment governed by increased gravity. In one of the pioneering sinkhole modelling studies, Terzaghi [11] investigated the stress distribution in sand above a yielding trapdoor which was followed by Costa et al. [12], Jacobsz [13] and Al-Naddaf [14]. Other studies include tests on sand slabs or beams spanning over openings to study sinkhole development [15–18].

Furthermore, conceptual 1-g models have been studied in China after many sinkhole collapses occurred. The physical models attempted to simulate the entire sinkhole formation process by simulating basic geologic conditions as well as hydrodynamic features [19]. A similar study by Jiang et al. [20] studied the effect of internal air pressure changes and groundwater level fluctuations on the deformational behaviour of the surface cover spanning over a cavity.

Limited literature is available pertaining to the monitoring of sinkhole formation using fibre optic technology. However, a study done by Briançon et al. [21] incorporated the use of FBGs to monitor possible soil subsidence underneath a railway through continuous real-time strain measurements.

### 3 Introduction to Optic Fibre Sensing Using FBGs

Optic fibre consists of a glass core, enclosed by a glass cladding that has a higher refractive index than the glass core. Electromagnetic energy propagates in the core of the optical fibre by means of total internal reflection.

An FBG sensor in an optic fibre is a periodic modulation of the refractive index of the glass core of the optic fibre. The periodic modulation, i.e. the Bragg grating, is imprinted into the optical fibre by UV laser irradiation. The FBG reflects a Bragg wavelength that depends on the refractive index of the sensor area and the period of the refractive index modulation [22].

The reflected Bragg wavelength of the FBG changes as the fibre is bent or if a temperature change is applied to it. Therefore, the fibre is sensitive to strain and temperature changes and this relationship is [23]:

$$\Delta\lambda/\lambda = \beta\varepsilon + \xi\Delta T \quad (1)$$

where  $\Delta\lambda$  is the change in wavelength of the reflected Bragg wavelength,  $\lambda$  is the original Bragg wavelength,  $\beta$  is the photo-elastic coefficient of the optic fibre,  $\varepsilon$  is the strain experienced by the FBG at a certain location,  $\xi$  is the thermo-optic coefficient for the optic fibre and  $\Delta T$  is the temperature change experienced by the FBG.

Optical fibre sensors can be multiplexed into a single optic fibre at predetermined locations and can measure in units of microstrain [10]. Another advantage of OFS is that the fibre sensors are small, can survive chemically aggressive environments and are immune to electromagnetic interference [4].

## 4 Testing Program

### 4.1 Similitude Laws in a 1-g Environment

Physical reduced-scale modelling requires that similitude laws need to be fulfilled because reduced-scale physical models have reduced soil volumes leading to smaller stress levels in the reduced-scale model as opposed to the prototype that is being simulated [24]. It should, however, be noted that there are some factors that could affect the similitude of the reduced-scale model and the prototype. These factors have been listed by Zornberg et al. [24] and they include a possible difference in stress paths between the model and the prototype, a difficulty of replicating compaction effects, and boundary effects such as friction and adhesion between the windows of the reduced-scale model and the soil. Thus, physical models cannot satisfy all similitude laws [25].

With this, larger prototype models can be represented by reduced-scale physical models through scaling factors which are tested under controlled conditions in a

controlled environment. Such models have been tested in a 1-g environment by numerous researchers [9, 25, 26]. Table 1 gives a summary of the scaling factors that need to be considered when performing scaled experimental work under normal gravitational conditions.

**Table 1.** Scaling factors for tests in a 1-g environment (after Ozkahriman and Wartman [7]).

Engineering properties	1-g Physical modelling scaling factors
Length and displacement	n
Soil density	1
Mass	$n^3$
Undrained shear strength	n
Time	$n^{0.5}$

## 4.2 Reduced-Scale Physical Model Description and Materials Tested

In this study, a reduced-scale model was used to simulate sinkhole formation and subsequent ground subsidence. The purpose of the test was to study the failure mechanism, and upwards propagation of the cavity. The use of OFSs allowed for strain and temperature measurements across the soil profile where the FBG sensors have been placed.

The reduced-scale physical model was constructed in a simulation box, made of Perspex, with inside dimensions of  $400 \times 80 \times 270$  mm high, representing a prototype soil mass measuring  $12 \times 2.4 \times 8.1$  m. The model scale was 1:30.

The tests were carried out on unreinforced cohesionless silica sand which comes from a commercial source in Cullinan, Gauteng. The poorly graded sand had a  $D_{50}$  particle diameter of 0.13 mm. The grading curve for the sand is displayed in Fig. 1. The sand had an angle of repose of about  $37^\circ$  and was placed and compacted in alternating layers of undyed sand (20 mm) and dyed sand (10 mm), in order to visualise the shape of the failure. The layers of sand were placed and compacted to a density of  $1560.98 \text{ kg/m}^3$  and four optic fibre cables with FBGs on each optic fibre cable were woven through the model at various depths. Twelve strain sensors (S1–S12) were multiplexed into 3 FBGs per fibre cable, 53 mm apart, to determine the strain in the centre of the zone of influence right above the cavity, as well as to determine the strain near the edges of the cavity as it propagates upwards. A temperature sensor, T, in a fifth fibre optic cable was also embedded into the model and positioned as illustrated in Fig. 2a.

The FBG sensors were manufactured in single mode photosensitive fibre in the Photonics Research laboratory of the University of Johannesburg using the phase mask technique and an Nd:YAG laser using the 266 nm wavelength. The FBG sensors were printed to reflect in the wavelength range between 1540 nm and 1555 nm.

The FBGs were calibrated for strain and temperature. Strain calibrations were done by stretching an FBG using a stepper motor which would stretch the sensor  $250 \mu$  at a time while measuring the corresponding change in wavelength. Temperature

calibrations were done by immersing an FBG into warm water of known temperature and measuring the corresponding change in wavelength as the water cooled down. The sensors were illuminated by a super-luminescent diode and the response was measured with an optical spectrum analyser (AQ6317C). The strain and temperature sensitivity were found to be  $1.2 \text{ pm}/\mu\epsilon$  and  $8.52 \text{ pm}/^\circ\text{C}$ , respectively.

A sinkhole was created by using a balloon filled with 440 ml of water to represent a cavity within the soil. The water-inflated balloon had a diameter of 93 mm (see Fig. 2b). The deflation of the balloon allowed for the upwards propagation of the sinkhole in two-dimensional plane-strain conditions [11]. The balloon was deflated by letting water out at a flow rate of 34.17 ml/min. The flow was regulated using a control valve and after 13 min the final diameter of the sinkhole that formed was 160 mm. This can be seen in Fig. 3 on the 100% plate.

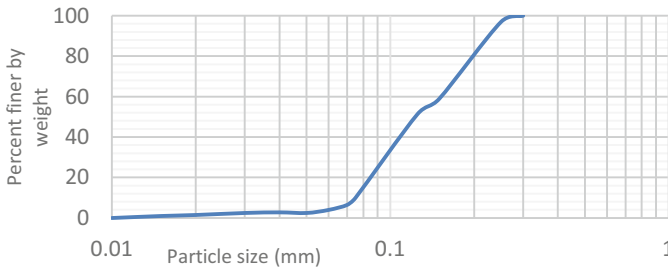


**Fig. 1.** Grading curve for the silica sand used in the experiment.

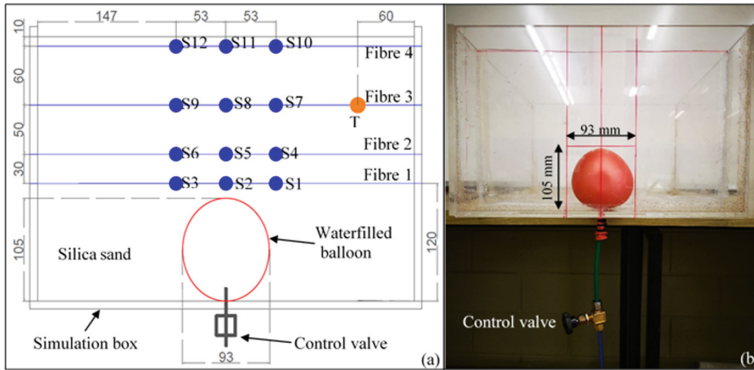


**Fig. 2.** (a) Elevation of the reduced-scale physical model setup showing the layout of the optic fibres, strain sensors (S1–S12) and the temperature sensor (T); (b) placement of the water-filled balloon before any sand was placed in the reduced-scale model. All measurements are in mm.

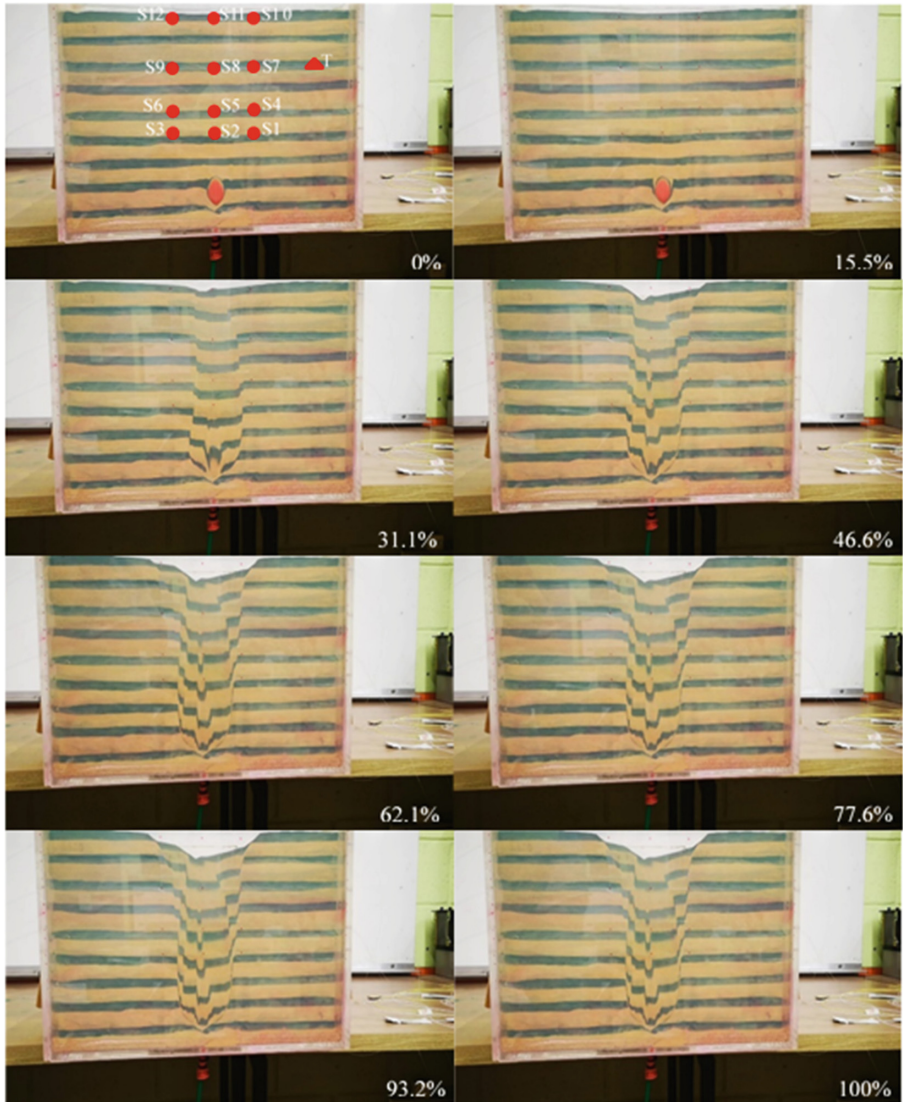


**Fig. 3.** Setup of the reduced-scale physical model showing the layout of the optic fibre strain sensors (S1–S12) and the temperature sensor (T) during testing.

## 5 Results

During testing, strain and temperature data were recorded using an HBM FS22 Industrial Braggmeter together with the BraggMonitor SI software. The test lasted 13 min and the development of the sinkhole is displayed in Fig. 3. The results for the 12 strain



sensors, compensated for temperature, are displayed in Figs. 4, 5, 6 and 7. The temperature at the start of the test was 23.2 °C and at the end of the test was 22.1 °C.

Optic fibre 1 contained strain sensors 1 to 3; optic fibre 2, strain sensors 4 to 6; optic fibre 3, strain sensors 7 to 9 and optic fibre 4, strain sensors 10 to 12.

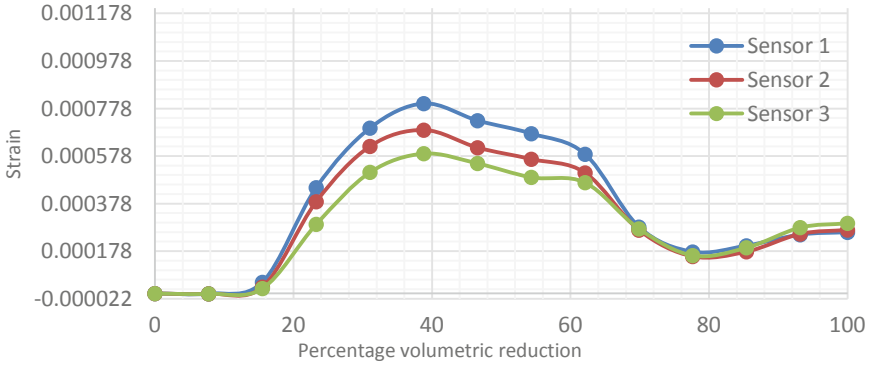


**Fig. 4.** Strain development in fibre 1 (sensors 1–3) as the volume of the balloon was reduced.

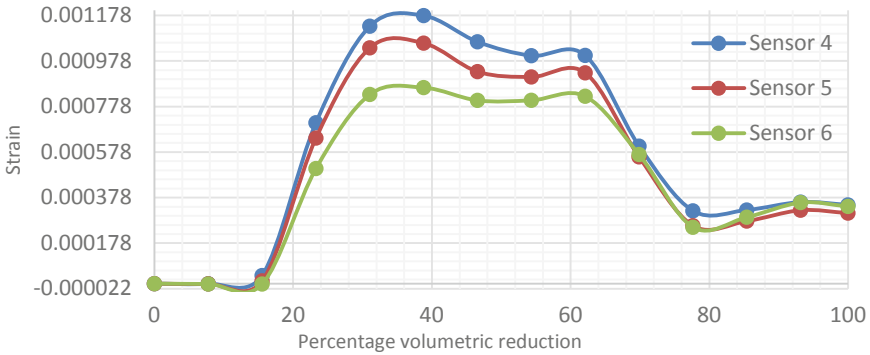


**Fig. 5.** Strain development in fibre 2 (sensors 4–6) as the volume of the balloon was reduced.

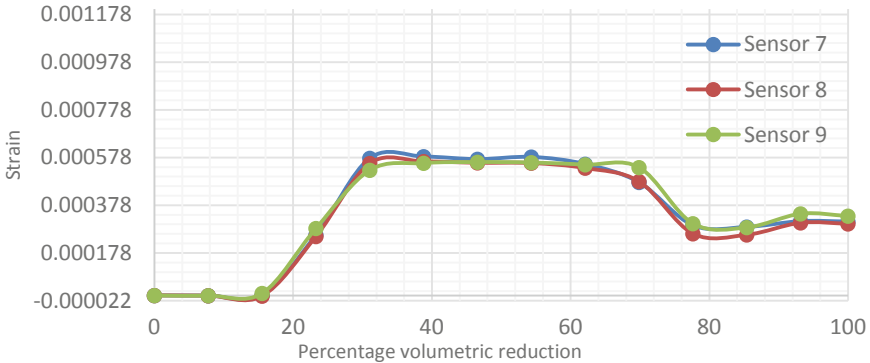


**Fig. 6.** Strain development in fibre 3 (sensors 7–9) as the volume of the balloon was reduced.



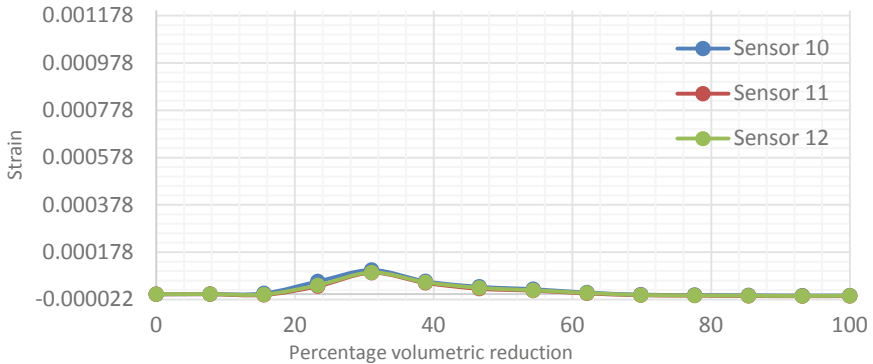


Fig. 7. Strain development in fibre 4 (sensors 10–12) as the volume of the balloon was reduced.

## 6 Discussion and Conclusion

In the current study, sinkhole development was studied using dry silica sand in a reduced-scale physical model using optic fibre sensors (FBGs). The study was conducted under normal gravity and the materials, model and sensors used are presented throughout the paper.

FBGs were manufactured using the phase mask method and were coated with an epoxy to ensure that the sensors were not damaged during testing. Twelve strain FBG sensors were inscribed into four optic fibres (three FBGs per fibre), 53 mm apart. The sensors were manufactured without any splices between the sensors. The FBGs were placed at predetermined locations in the various soil layers (see Fig. 2a) and were pre-stained to measure expansion and compression during testing. Temperature and strain data were obtained from the FBGs and were continuously logged throughout the test using an optical interrogator.

A cavity, represented by a water-filled balloon, deflated at a controlled rate, allowed for the upwards propagation of the cavity by creating a downward movement of the soil directly above the cavity, resulting in a sinkhole. Strain data displayed in Figs. 4, 5, 6 and 7 show the development of strains in various soil layers as the water-filled balloon was deflated and a sinkhole started forming.

After the commencement of volume reduction, the strain results show that maximum strain was experienced at a volume reduction between 31.1% and 38.8% in the model. The results obtained from the test showed that the highly sensitive sensors indicated that maximum strains occurred before maximum surface deformation was visually observed. Figure 3 can be compared to Figs. 4, 5, 6 and 7 at the various volumetric reduction percentages to illustrate how the strains developed in the various soil layers over time. It can also be seen from Fig. 3, on the 31.1% plate, that the propagation of the sinkhole narrowed upwards. It was observed by Jacobsz [11], that actual sinkholes are often narrower near the surface shortly after they appear. The width of the sinkhole shaft, evident below the sinkhole itself in the dark and light-coloured sand layers, shows that the width of the shaft is approximately equal to the width of the cavity.

Strain sensors S2, S5, S8, and S11 were placed in the centre of the model, directly above the cavity and the remainder of the strain sensors were positioned on both sides, slightly wider than the width of the cavity. The reason for that was to determine if the strains experienced by the strain sensors in the centre of the model would be similar to the strains experienced by the strain sensors placed on the sides of the cavity. From the results, it can be seen that the strain experienced by the FBG sensors are all similar, but strain sensors S1, S4, S7 and S10, to the right side of the balloon, experienced larger strains. This could be because the FBG sensors were placed slightly off-centre. It is, however, evident that the strain sensors closest to the surface experienced the smallest strains since the deflation of the balloon allowed the cavity to propagate towards the surface which reduced the vertical stress in the sand above it. None of the sensors failed or were damaged during the test, showing that this instrumentation is suitable for use in physical model studies.

Further testing is planned in a geotechnical centrifuge to allow strain development above propagating sinkholes to be studied at prototype stress levels. In addition, future studies will include studying the effect of abutments to simulate rock pinnacles against which the arch can thrust during cavity propagation.

**Acknowledgements.** This work has been supported by Telkom SA SOC Ltd., CBI-Electric, the National Laser Centre (NLC) and the National Research Foundation of South Africa (NRF).

## References

1. Jennings, J.E., Brink, A.B., Louw, A., Gowan, G.D.: Sinkholes and subsidences in the Transvaal dolomite of South Africa. In: Proceedings of the 6th International Conference on Soil Mechanics and Foundation Engineering, Montreal, University of Toronto, pp. 51–54 (1965)
2. Oosthuizen, A.C., van Rooy, J.L.: Hazard of sinkhole formation in the Centurion CBD using the simplified method of scenario supposition. *J. South Afr. Inst. Civ. Eng.* **57**(2), 69–75 (2015)
3. Soga, K., Schooling, J.: Infrastructure sensing. *Interface Focus* **6**(4), 20160023 (2016)
4. Chtcherbakov, A.A.: Reflective Interferometric Fibre Optic Sensors. University of Johannesburg, Johannesburg (1997)
5. Wang, B., Li, K., Wei, G.: Test on application of distributed fiber optic sensing technique into soil slope monitoring. *J. Int. Consort. Landslides* **6**(1), 61–68 (2008)
6. Picarelli, L., Damiano, E., Greco, G., Minardo, A., Olivares, L., Zeni, L.: Performance of slope behaviour in unsaturated pyroclastic soils. *J. Mt. Sci.* **12**(6), 1434–1447 (2015)
7. Ozkahriman, F., Wartman, J.: Investigation of 1-g Similitude Laws by “Modeling-of-Models” Exercise. Denver, Colorado (2007)
8. Wartman, J.: Geotechnical physical modeling for education: learning theory approach. *Prof. Issues Eng. Educ. Pract.* **132**(4), 288–296 (2006)
9. Zhu, H., Wang, Z., Wong, J.K.: Feasibility study of strain based stability evaluation of locally loaded slopes: insights from physical and numerical modeling. *Eng. Geol.* **208**, 39–50 (2016)
10. Kapogianni, E., Sakellariou, M., Laue, J.: Experimental investigation of reinforced soil slopes in a geotechnical centrifuge, with the use of optical fibre sensors. *Geotech. Geol. Eng.* **35**(2), 585–605 (2016)

11. Terzaghi, K.: Stress distribution in dry and saturated sand above a yielding trap-door. In: Proceedings of the 1st International Conference on Soil Mechanics. Harvard University, Cambridge (1936)
12. Costa, Y.D., Zornberg, J.G., Bueno, B.S., Costa, C.L.: Failure mechanisms in sand over a deep active trapdoor. *J. Geotech. Geoenviron. Eng.* **135**(11), 1741–1753 (2009)
13. Jacobsz, S.W.: Trapdoor experiments studying cavity propagation. In: Proceedings of the first Southern African Geotechnical Conference, Sun City, South Africa (2016)
14. Al-Naddaf, M., Han, J., Jawad, S., Abdulrasool, G., Xu, C.: Investigation of stability of soil arching under surface loading using trapdoor model tests. In: Proceedings of the 19th International Conference on Soil Mechanics and Geotechnical Engineering, Seoul (2017)
15. Craig, W.H.: Collapse of cohesive overburden following removal. *Can. Geotech. J.* **27**(3), 355–364 (1990)
16. Abdulla, W.A., Goodings, D.J.: Modeling of sinkholes in weakly cemented sand. *J. Geotech. Eng.* **122**(12), 998–1005 (1996)
17. Goodings, D.J., Abdulla, W.A.: Stability charts for predicting sinkholes in weakly cemented sand over Karst limestone. *Eng. Geol.* **65**(2–3), 179–184 (2002)
18. Bronkhorst, W.P., Jacobsz, S.W.: The behaviour of weakly cemented sand beams spanning over openings. In: 8th International Conference on Physical Modelling in Geotechnics, Perth, Australia (2014)
19. Lei, M., Jiang, X., Yu, L.: New advances in Karst collapse in China. *Environ. Geol.* **42**(5), 462–468 (2002)
20. Jiang, X., Gao, Y., Wu, Y., Lei, M.: Use of Brillouin optical time domain reflectometry to monitor soil-cave and sinkhole formation. *Environ. Earth Sci.* **75**(225), 1–8 (2016)
21. Briançon, L., Nancey, A., Robinet, A., Voet, M.: Set up of a warning system integrated inside a reinforced geotextile for the survey of railway. In: 8th International Conference on Geosynthetics, Yokohama, Japan (2006)
22. Huang, L., Liu, F., Li, J.: Slope detection based on grating sensors. *iJOE* **14**(11), 147–159 (2018)
23. Udd, E., Spillman Jr., W.: *Fiber Optic Sensors*, 2nd edn. Wiley, New Jersey (2011)
24. Zornberg, J.G., Mitchell, J.K., Sitar, N.: Testing of reinforced slopes in a geotechnical centrifuge. *Geotech. Test. J.* **20**(4), 470–480 (1997)
25. Ni, P., Wang, S., Zhang, S., Mei, L.: Response of heterogenous slopes to increased surcharge load. *Comput. Geotech.* **78**, 99–109 (2016)
26. Palmeira, E.M., Gomes, R.C.: Comparisons of predicted and observed failure mechanisms in model reinforced soil walls. *Geosynth. Int.* **3**(3), 329–347 (1996)